Tan, C. M., Beach, M. A., & Nix, A. R. (2002). Multi-dimensional DFT beamspace SAGE super-resolution algorithm. In Sensor Array and Multichannel Signal Processing Workshop, 2002. (pp. 475 - 479). Institute of Electrical and Electronics Engineers (IEEE).

MULTI-DIMENSIONAL DFT BEAMSPACE SAGE SUPER-RESOLUTION ALGORITHM

C. M. Tan, M.A. Beach, A.R. Nix

Centre for Communications Research
University of Bristol, Bristol BS8 1UB, UK.
Tel: +44 (0)117 954 5202, Fax: +44 (0)117 954 5206

ABSTRACT

A novel multi-dimensional frequency domain SAGE algorithm in DFT beamspace for estimating channel parameters is presented. In contrast to the classical implementation of the SAGE algorithm in element space, the proposed algorithm allows the estimates of each parameter to be optimised within a smaller domain. Further reduction in the computational complexity within each SAGE iteration is achieved since the *alternating parameters* in the correlation process are in the real-valued domain. A major advantage of the proposed algorithm is its ability for mapping onto parallel processors. In this paper, the general implementation of the proposed algorithm with efficient matrix computation is presented, with conditions necessary for achieving the best performance stated. Finally, its performance is evaluated by using the real channel measurement data.

1. INTRODUCTION

Motivated by the need to shatter the classical Fourier limitation, numerous super-resolution algorithms have been developed to estimate channel parameters. In general, the development and fundamental philosophy of the algorithms may be classified into two major groups based on eigen-decomposition and maximum-likelihood.

The most commonly used Estimation of Signal Parameters via Rotational Invariance Techniques (ESPRIT) and MUtiple SIgnal Classification (MUSIC) algorithms are based on eigen-decomposition. One of the strict conditions imposed is that the array must exhibit the Vandermonde structure in its steering vector so that subarray-smoothing can be applied to cope with the correlated signals. On the other hand, one of the maximum-likelihood-based algorithms, namely the Space-Alternating Generalised Expectation-Maximisation (SAGE) algorithm, has more flexibility in the array geometry. It is applicable (in theory) to any arbitrary array geometry, provided that exact knowledge of the array manifold is available. However, despite the improved convergence speed of the SAGE algorithm compared to the Maximum-Likelihood Estimator and Expectation-Maximisation algorithms, the major drawback of these algorithms persists, i.e. a long processing time. This is inevitable since these algorithms are iterative in nature.

Here, a novel implementation of the SAGE algorithm in the frequency domain and DFT beamspace is proposed in an attempt to reduce the processing time of the classical SAGE algorithm by a few orders. It allows the estimates of each channel parameter to be optimised with a data size of reduced dimensionality. In addition, the computations in the SAGE iterations are much simplified since the *alternating parameters* associated with the correlation process are in the real-valued domain. This significantly reduces the processing power needed in the iterations.

The proposed algorithm retains all the advantages of the classical SAGE algorithm, while being able to reduce the computational complexity, memory consumption, and processing time after the element-space-to-beamspace transformation. One major advantage of the proposed algorithm is its amenability to parallel processing in digital hardware. Note that the proposed algorithm can only fully exploit all these extra advantages if *a priori* knowledge of the channel is available.

This paper is organised as follows. Section 2 describes the channel model used in the development of the multi-dimensional frequency domain DFT beamspace SAGE algorithm. Section 3 presents the general implementation of the proposed algorithm. Section 4 discusses the conditions necessary to obtain the optimum performance. Section 5 demonstrates its performance and Section 6 concludes this paper.

2. MULTI-DIMENSIONAL CHANNEL MODEL

The multi-dimensional channel model developed in this section is based on the Medav RUSK channel sounder [1], but it is generic to all situations. Within some limited time frame and assuming a wide-sense stationary process, the channel may be described by a stationary Doppler-delay-azimuth-variant impulse response (1):

$$h(\nu,\tau,\theta)=\sum_{l=1}^{L}\Gamma_l(\nu_l)\cdot\delta(\nu-\nu_l)\cdot\delta(\tau-\tau_l)\cdot\delta(\theta-\theta_l) \quad (1)$$

0-7803-7551-3/02/$17.00 ©2002 IEEE

where v is the Doppler frequency, τ is the delay, θ is the azimuth angle (from the antenna array broadside), Γ is the path weight and L is the number of multipaths. For the frequency domain implementation of the proposed algorithm, (1) may be described by a time-space-variant frequency channel response (2),

$$H(t,f,s)=\sum_{l=1}^{L}\gamma_l(t)\cdot e^{-j2\pi v_l}\cdot e^{-j2\pi f\tau_l}\cdot e^{-j2\pi s u_l} \qquad (2)$$

where γ is the path weight, u = sin(θ), and t, f and s represent the time, frequency, and spatial domains sample.

Effectively, (2) represents a 3-D channel model consisting of L undamped exponential modes and the parameter estimation process is equivalent to a 3-D harmonic retrieval problem. Since the R-dimension (R-D) estimation process requires the use of an R-D array, the channel can be generally modelled as

$$H_{k_1,k_2,\cdots,k_R}=\sum_{l=1}^{L}\left(\gamma_l\prod_{r=1}^{R}e^{-jk_r\mu_l^{(r)}}\right)+N_{k_1,k_2,\cdots,k_R} \qquad (3)$$

where $k_r\in[1,K_r]$ is the entry of the R-D array, K_r is the number of elements in the r-th dimension array, and N is the complex Additive White Gaussian Noise (AWGN). For the case of (2), $\mu_l^{(v)}=2\pi\Delta t v_l$, $\mu_l^{(\tau)}=2\pi\Delta f\tau_l$, and $\mu_l^{(\theta)}=2\pi\Delta s\sin(\theta)$, where Δt, Δf, and Δs are the spacing between the elements in the time, frequency, and spatial domains, respectively. Note that the Shannon sampling theorem must hold, i.e. $\Re\{\mu_l^{(r)}\}\in[0,2\pi]$ must be fulfilled, where $\Re\{\cdot\}$ represents the range space of the argument. This condition is crucial to guarantee the successful estimation of each parameter.

In order to facilitate an efficient matrix computation in the proposed algorithm, the R-D channel response matrix, $\mathbf{H}$, is represented as a vector through the $vec\{.\}$ operator that maps an R-D matrix into a $\left(\prod_{r=1}^{R}K_r\right)$x1 column vector by stacking the columns of the matrix.

$$\mathbf{x}=vec\{\mathbf{H}\}$$
$$=\sum_{l=1}^{L}\gamma_l\cdot\mathbf{a}(\mu_l^{(R)})\otimes\cdots\otimes\mathbf{a}(\mu_l^{(2)})\otimes\mathbf{a}(\mu_l^{(1)})+\mathbf{n} \qquad (4)$$

where $\mathbf{n}=vec\{\mathbf{N}\}$, $\otimes$ denotes the Kronecker product, and the r-th dimension steering vector (by taking the array centre as reference) is given by:

$$\mathbf{a}(\mu_l^{(r)})=e^{j\frac{K_r-1}{2}\mu_l^{(r)}}\left[1,e^{-j\mu_l^{(r)}},e^{-j2\mu_l^{(r)}},\cdots,e^{-j(K_r-1)\mu_l^{(r)}}\right]^T \qquad (5)$$

where the superscript T denotes the vector transposition.

3. GENERAL IMPLEMENTATION OF THE PROPOSED ALGORITHM

3.1. Beamspace transformation

Note that the channel model in (4) represents the element space model where the data size is given by $\left(\prod_{r=1}^{R}K_r\right)$x1. Reduced dimensionality in the data size is achieved by transforming the data (K x 1) from the element space into the beamspace domain of a smaller size (B x 1, $B < K$). This transformation process is accomplished by pre-multiplying the data with a DFT beamforming matrix that is able to form B consecutive orthogonal beams in the sector of interest, namely the m-th band. Figure 1 shows the 7 consecutive orthogonal beams formed at the region of ±40° with a 10-element uniform linear array (ULA). Thus the data size is reduced from 10 to 7 and the subsequent processing can be concentrated in the region of ±40°.

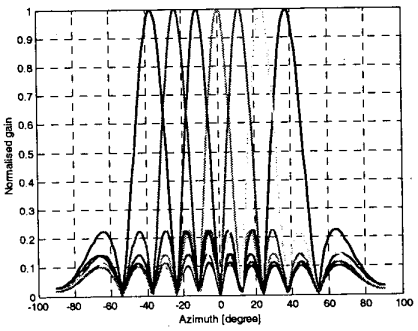

Figure 1. Illustration of the orthogonal beamforming

The r-th dimension scaled DFT beamforming vector is defined as [3]:

$$\mathbf{w}^{(r)}(\beta)=e^{-j\frac{K_r-1}{2}\pi\beta}\left[1,e^{j\pi\beta},e^{j2\pi\beta},\cdots\cdots,e^{j(K_r-1)\pi\beta}\right]^T \qquad (6)$$

and the corresponding (K_r x B_r) beamforming matrix for the m-th band is defined as:

$$\mathbf{W}_m^{(r)}=\left[\mathbf{w}^{(r)}\left(m\frac{2}{K_r}\right)\vdots\mathbf{w}^{(r)}\left([m+1]\frac{2}{K_r}\right)\vdots\cdots\cdots\right.$$
$$\left.\cdots\cdots\vdots\mathbf{w}^{(r)}\left([m+B_r-1]\frac{2}{K_r}\right)\right] \qquad (7)$$

where B_r is the number of consecutive orthogonal beams in the r-th dimension to be formed in the m-th band, $B_r<K_r$. The overall R-D DFT beamforming matrix is given by:

$$\mathbf{W}_m^{(R-D)}=\mathbf{W}_m^{(R)}\otimes\cdots\cdots\otimes\mathbf{W}_m^{(2)}\otimes\mathbf{W}_m^{(1)} \qquad (8)$$

and the beamspace transformation is accomplished by (9):

$$\mathbf{y}_m = \mathbf{W}_m^{(R-D)^H}\mathbf{x} \tag{9}$$

where the superscript 'H' denotes the Hermitian transposition. With this transformation into the m-th band in beamspace, we have reduced the original data size from $\left(\prod_{r=1}^{R} K_r\right)$x1 to $\left(\prod_{r=1}^{R} B_r\right)$x1, where $B_r < K_r$. All the subsequent signal processing can thus be performed in a reduced dimensionality.

3.2. *R*-D DFT beamspace SAGE algorithm

Although the input data at this stage is in the DFT beamspace frequency domain, the basic implementation of the R-D DFT beamspace SAGE algorithm is still similar to the classical SAGE algorithm [4] in the element space. Each iteration consists of the *Expectation*-step (E-step) and the *Maximisation*-step (M-step). Since the signal processing in this section is devoted to the beamspace data in the m-th band, the subscript 'm' is dropped off from this point onwards to simplify the notation.

In the E-step, the *complete data* of the l-th path, $\hat{\mathbf{z}}_l$, can either be obtained by using the parallel interference cancellation (PIC) or the successive interference cancellation (SIC) technique, given by (10) and (11), respectively:

$$\hat{\mathbf{z}}_{l,\langle PIC\rangle} = \mathbf{y} - \sum_{\substack{l'=1 \\ l' \neq l}}^{L} \hat{\mathbf{s}}_{l'} \tag{10}$$

$$\hat{\mathbf{z}}_{l,\langle SIC\rangle} = \mathbf{y} - \sum_{l'=1}^{l-1} \hat{\mathbf{s}}_{l'} \tag{11}$$

where $\hat{\mathbf{s}}_l$ is the beamspace signal copy of the l-th path (17), and $\hat{\chi}$ denotes the estimation for χ.

In the M-step, the parameters of the l-th path are estimated sequentially by performing the *coordinate-wise-updating procedure*. This is performed by searching for the peak in the corresponding r-th dimension 1-D correlation function (15) in a sequential manner for all the R parameters associated with the l-th path. The r-th dimension argument that corresponds to the peak in the correlation function can be related to the corresponding r-th dimension channel parameter value, as described in Section 2. This is illustrated as follows.

$$\mu_l^{(1)''} = \arg \max_{\mu_l^{(1)}} \left\{ \left| f\left(\mu_l^{(1)}, \mu_l^{(2)'}, \cdots, \mu_l^{(R)'}\right) \right| \right\} \tag{12}$$

$$\mu_l^{(2)''} = \arg \max_{\mu_l^{(2)}} \left\{ \left| f\left(\mu_l^{(1)''}, \mu_l^{(2)}, \cdots, \mu_l^{(R)'}\right) \right| \right\} \tag{13}$$

$$\vdots$$

$$\mu_l^{(R)''} = \arg \max_{\mu_l^{(R)}} \left\{ \left| f\left(\mu_l^{(1)''}, \mu_l^{(2)''}, \cdots, \mu_l^{(R)}\right) \right| \right\} \tag{14}$$

where the correlation function is given by:

$$f\left(\mu_l^{(1)}, \cdots, \mu_l^{(R)}\right) = \left[\mathbf{b}\left(\mu_l^{(R)}\right) \otimes \cdots\cdots \otimes \mathbf{b}\left(\mu_l^{(2)}\right) \otimes \cdots \cdots \mathbf{b}\left(\mu_l^{(1)}\right)\right]^T \hat{\mathbf{z}}_l \tag{15}$$

$\mu_l^{(r)''}$ denotes the newly updated r-th dimension argument in the current iteration, $\mu_l^{(r)'}$ is the previously updated argument in the last iteration, and the beamspace steering vector, $\mathbf{b}(\cdot)$, is given by:

$$\mathbf{b}\left(\mu_l^{(r)}\right) = \mathbf{W}^{(r)H}\mathbf{a}\left(\mu_l^{(r)}\right) \tag{16}$$

Note that the element space steering vector, $\mathbf{a}\left(\mu_l^{(r)}\right)$, and the beamspace transformation matrix, $\mathbf{W}^{(r)}$, are both column conjugate symmetric. It thus follows that the corresponding beamspace steering vector, $\mathbf{b}\left(\mu_l^{(r)}\right)$, is real-valued through the operation of (16), which can be performed and stored into the processor's memory prior to each iteration. Hence, the computational load of the correlation process can be reduced significantly (especially in a multi-dimensional case), resulting in a more efficient implementation with reduced demand for high processing power. Better memory management can also be achieved since only the real-valued beamspace steering vectors need to be stored, instead of the complex-valued element space steering vectors.

The signal copy of the l-th path, which is required in the E-step, is thus given by:

$$\hat{\mathbf{s}}_l = \gamma_l \cdot \mathbf{b}\left(\mu_l^{(R-D)''}\right) \tag{17}$$

$$\gamma_l = \mathbf{b}\left(\mu_l^{(R-D)''}\right)^{+} \hat{\mathbf{z}}_l \tag{18}$$

$$\mathbf{b}\left(\mu_l^{(R-D)''}\right) = \mathbf{b}\left(\mu_l^{(R)''}\right) \otimes \cdots \otimes \mathbf{b}\left(\mu_l^{(2)''}\right) \otimes \mathbf{b}\left(\mu_l^{(1)''}\right) \tag{19}$$

where $\mathbf{b}(\cdot)^{+}$ represents the Moore-Penrose pseudoinverse of $\mathbf{b}(\cdot)$, and γ_l is the l-th signal path weight.

The E-step and M-step described above are executed sequentially for each of the L paths in iterations. The iteration is stopped when the convergence is achieved, i.e. the estimated channel parameters have reached a steady state in which their values do not change anymore (within a pre-defined threshold) for several iterations. More iterations are needed if the paths are coherent and the parameters are closely spaced.

3.3. Initialisation of the algorithm

From our experience with the SAGE algorithm, we found that the performance and the convergence speed are highly sensitive to the way it is initialised. With a zero (i.e. all parameters are set to zero) or random initialisation, instability occurs occasionally in the implementation in which the algorithm diverges from the steady state instead of converging to it. More iterations are also needed in order to achieve convergence.

Here, we propose the SIC technique in conjunction with the *incoherent combining procedure* as the initialisation of the proposed algorithm. The *alternating parameter* of the higher dimension is set to zero (*incoherently combining*) when the parameter of the lower dimension is being initialised.

$$\mu_l^{(1)''} = \arg \max_{\mu_l^{(1)}} \left\{ \left| f\left(\mu_l^{(1)}, \mu_l^{(2)'} = 0, \cdots, \mu_l^{(R)'} = 0 \right) \right| \right\} \quad (20)$$

$$\mu_l^{(2)''} = \arg \max_{\mu_l^{(2)}} \left\{ \left| f\left(\mu_l^{(1)''}, \mu_l^{(2)}, \cdots, \mu_l^{(R)'} = 0 \right) \right| \right\} \quad (21)$$

After the initialisation for all the R parameters associated with the l-th path, its signal copy is reconstructed and subtracted from $\hat{\mathbf{z}}_{l+1}$ with the SIC scheme (11). This procedure continues until all R parameters in all L paths have been initialised. It provides a coarse estimate of the parameters. Fine-tuning and super-resolution is achieved through the SAGE iterations until it converges.

3.4. Determination of the model order

We found that in a multi-dimensional case, the determination of the model order using the Akaike Information Criterion (AIC) and the Minimum Description Length (MDL) [5] provides highly unreliable results. Hence, we propose to set L to a certain number (50 say, in a multipath-rich environment) as an initial guess. The model order is then determined by setting a threshold in the calculated γ (18) values. The l-th path will be rejected as noise if γ_l is beyond the threshold window set in the algorithm. This method ensures that all the dominant multipaths in the channel (within the m-th band) are extracted by the algorithm. Note that this technique is currently widely used by many researchers in this field.

3.5. Parallel processing

Due to the inherent property of the beamspace processing, different R-D subbands could be formed with different R-D beamspace transformation matrices. The sectorisation of the R-D data into different R-D regions of a smaller size allows all sectors to be processed in parallel using the proposed algorithm. This feature is beneficial if SAGE were to be implemented in digital hardware. A lower computational complexity and lesser memory consumption of the proposed algorithm make it more feasible for real time applications. However, due to space limitation, the implementation of this feature is not addressed here.

4. CONDITIONS FOR OPTIMUM PERFORMANCE

Note that the model described in Section 2 assumes that the impinging signals are narrowband, i.e. $\frac{B_w}{f_c} < 0.1$, where B_w is the bandwidth, and f_c is the carrier frequency. This is important in direction finding and the antenna array must be placed in the far-field region. A rule of thumb for the far-field is $\frac{2D^2}{\lambda}$, where λ is the carrier wavelength, and D is the antenna array dimension. In addition, the antenna array and the measurement system must be properly calibrated to eliminate any disturbance that might cause errors in the estimation.

Since the noise is spatially white across the R-D aperture, the signal-to-noise-ratio (SNR) can be enhanced with more data snapshots fed into the algorithm. However, all the snapshots must be taken well within the coherence time of the channel and the measurement equipment must be able to support this. Better accuracy and less iteration can be achieved with more number of elements across the arrays (in temporal, frequency, or spatial domains) since more degrees of freedom are available.

The degree of accuracy and super-resolution capability of the algorithm also depends on the quantisation (discretisation) of the arguments used to determine the peak in the correlation function. Better accuracy could be obtained with a finer quantisation grid at the cost of increased processing time. A dynamic argument quantisation technique may be used to assign different quantisation grids to different iteration runs.

Since the signal processing is concentrated in the m-th band, any dominant signals beyond the m-th band might affect the accuracy of the parameters estimation corresponding to the in-band signals. A windowing function can be applied to reduce the out-of-band sidelobes of the beams and hence any out-of-band signal can be suppressed efficiently. The beams must also exhibit common nulls throughout the entire sector. Note that this procedure is crucial in parallel processing of the proposed algorithm. However, its implementation is not discussed here due to space limitation.

5. PERFORMANCE EVALUATION

Here, we use the proposed algorithm to estimate the channel parameters from the real measurement data so that its performance can be evaluated in a more realistic way. We can also assess the validity of the mathematical model developed in Section 2, which was used in the development of this algorithm. The real physical channel model must closely match the mathematical model. Otherwise, poor resolution and consistent errors would occur due the *model-mismatch* problem.

The measurement was conducted at 2.12 GHz using a Medav RUSK BRI channel sounder [1] in an anechoic chamber. The transmitted signal bandwidth was 20 MHz. An 8-element ULA with 0.563λ element spacing (Δs) was used to receive signals from 2 coherent sources separated by 20°. The sources were set to face the ULA at the same height (Figure 2). One of the coherent sources was moved forward and backward by fractions of a wavelength in each ULA's orientation to create multiple samples of different phase shifts at the ULA. The ULA was rotated from –30° to 30° in 10° steps. It was confined to ±30° to avoid the ambiguity problem in direction-of-arrival (DoA) estimation, since $\Delta s > 0.5\lambda$.

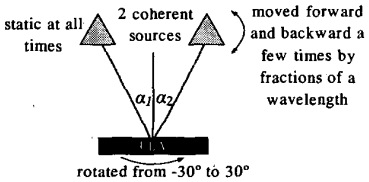

Figure 2. Test measurement setup

We used the 3-D DFT beamspace SAGE algorithm to estimate the DoA, time-delay-of-arrival (TDoA) and the Doppler frequency. The 3-D beams were confined to ±50° and 0-100 ns region to reduce the complexity. The results were compared with that of the classical 3-D SAGE and 3-D beamspace Unitary ESPRIT [2] (with 2-D subarray-smoothing) algorithms. Figure 3 shows the results of the estimated DoA (α_1 and α_2). It is shown that all the results are very similar to each other. We found that the PIC outperforms the SIC in this case. In SIC, the dominant waves are estimated and suppressed one-by-one, but $\hat{\mathbf{z}}_{l,\langle SIC\rangle}$ still contains other paths that have not been suppressed from $\hat{\mathbf{z}}_{l,\langle SIC\rangle}$ and this will affect the correlation process during the l-th run within the iteration. Since L=2 in this measurement, the presence of the second dominant source in $\hat{\mathbf{z}}_{1,\langle SIC\rangle}$ has caused the estimation to have a larger variance. However, the second path is suppressed from $\hat{\mathbf{z}}_{1,\langle PIC\rangle}$. Thus, the correlation in PIC can be performed without the influence of any other path (hence the improved performance). Due to space limitations, the estimated TDoA and Dopper frequency are not shown here. The TDoA values are very consistent and their variance is less than 5 ns (Rayleigh resolution is 50 ns). The Doppler was zero at all times inside the chamber.

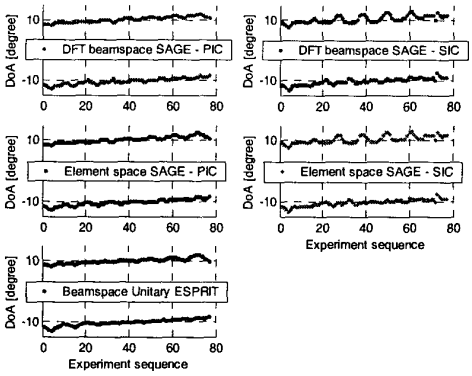

Figure 3. Estimated DoA results with different algorithms

6. CONCLUSIONS

A novel implementation of the SAGE algorithm in DFT beamspace has been presented and the conditions needed for its optimum performance stated. The proposed algorithm is able to reduce the computational burden, memory consumption, and the processing time of the classical SAGE algorithm through the element-space-to-beamspace transformation and efficient matrix computation. Like other super-resolution algorithms, the proposed algorithm is robust and able to produce reliable and accurate results.

ACKNOWLEDGEMENT

The authors would like to acknowledge the Mobile VCE (www.mobilevce.com) for the financial support of C. M. Tan, Technical University Ilmenau (Germany) for the use of their equipment, and Allgon System AB for the loan of their 2 GHz UMTS-FDD panel array.

REFERENCES

[1] R. S. Thomä, D. Hampicke, A. Richter, G. Sommerkorn, A. Schneider, U. Trautwein, W. Wirnitzer, "Identification of time-variant directional mobile radio channels," *IEEE Trans. Instrum. and Meas.*, vol. 49, pp. 357–364, April 2000.

[2] M. Haardt, "*Efficient one-, two-, and multidimensional high-resolution array signal processing*," PhD. Thesis, ISBN 3-8265-2220-6, 1996.

[3] M. D. Zoltowski, G. M. Kautz, S. Silverstein, "Beamspace Root-MUSIC," *IEEE Trans. SP*, vol. 41, pp. 344-364, January 1993.

[4] B. H. Fleury, M. Tschudin, R. Heddergott, D. Dahlhaus, K. I. Pedersen, "Channel parameter estimation in mobile radio environments using the SAGE algorithm," *IEEE JSAC*, vol. 17, pp. 434-449, March 1999.

[5] M. Wax, T. Kailath, "Detection of signals by information theoretic criteria," *IEEE Trans. ASSP*, vol. 32, pp. 387-392, April 1985.